

## II.G.6 Photoelectrochemical Materials: Theory and Modeling

Yanfa Yan (Primary Contact), Wanjian Yin, Muhammad Huda, Su-Huai Wei, Mowafak Al-Jassim, and John Turner  
National Renewable Energy Laboratory  
1617 Cole Blvd.  
Golden, CO 80401  
Phone: (303) 384-6456  
E-mail: Yanfa.Yan@nrel.gov

DOE Technology Development Manager:  
Eric Miller  
Phone: (202) 287-5829  
E-mail: Eric.Miller@hq.doe.gov

Project Start Date: 2007  
Project End Date: Project continuation and direction determined annually by DOE

### Objectives

The main focus of the project is to:

- Understand the performance of current photoelectrochemical (PEC) materials.
- Provide guidance and solution for performance improvement.
- Design and discover new materials.
- Provide theoretical basis for go/no-go decisions to DOE PEC H<sub>2</sub> projects.

### Technical Barriers

This project addresses the following technical barriers from the Production section of the Hydrogen, Fuel Cells and Infrastructure Technologies Program Multi-Year Research, Development and Demonstration Plan:

- (Y) Materials Efficiency
- (Z) Materials Durability
- (AB) Bulk Materials Synthesis

### Technical Targets

This project is intended to provide a theoretical understanding of the performance of current PEC materials and provide feedback and guidance for performance improvement.

### Accomplishments

- Studied theoretically the properties of Cu delafossite (CuXO<sub>2</sub>, X= group-IIIA, or IIIB) materials for PEC water splitting.
- Proposed solution for enhancing the optical absorption for Cu delafossite through symmetry breaking.
- Investigated the effects of W doping in BiVO<sub>4</sub>, a potential material for PEC water splitting.



### Introduction

Cu delafossites, CuMO<sub>2</sub> (M = group-III elements), have received great attention in recent years due to their potential applications as electrodes for hydrogen production by PEC water splitting and transparent conductive oxides (TCOs) in optoelectronic devices [1,2]. The p-type conductivity and good hole mobility are what make the Cu delafossites so unique and more attractive in these applications than other metal oxides. For instance, due to their p-type nature, the Cu delafossites are resistive against oxidative corrosion. Some recent experimental studies demonstrated that Cu delafossites are stable in solution and are capable of H<sub>2</sub> evolution from water [1,2].

Among the two Cu delafossite families, [CuM<sup>IIIA</sup>O<sub>2</sub> (M<sup>IIIA</sup>=Al, Ga, In) and CuM<sup>IIIB</sup>O<sub>2</sub> (M<sup>IIIB</sup>=Sc, Y, La)], the CuM<sup>IIIA</sup>O<sub>2</sub> family (particularly M<sup>IIIA</sup>=Al) has mostly been considered for p-type TCOs. On the other hand, the focus on the CuM<sup>IIIB</sup>O<sub>2</sub> family has been limited and specifically on the application on H production by solar water splitting. Until now, there has been no solid understanding of which family is better suited for which of the applications.

Despite the similar structures, the CuM<sup>IIIA</sup>O<sub>2</sub> and CuM<sup>IIIB</sup>O<sub>2</sub> families exhibit significantly different electronic properties. The optical measurements indicate that the group-IIIA delafossite family has indirect bandgaps [3,4], and can hardly be doped p-type by extrinsic dopants [5]. On the other hand, the group-IIIB delafossite family has been exclusively reported to have direct wide bandgaps and can be doped by extrinsic dopants.

It is also important to note that the main difference between the requirements for PEC electrodes and TCOs is as follows: PEC electrodes require smaller bandgaps (in the visible region) and an appropriate band-edge alignment, whereas TCOs require larger bandgaps (in the ultraviolet region). We therefore needed to conduct

a detailed comparative study on the electronic structure between the  $\text{CuM}^{\text{IIIA}}\text{O}_2$  and  $\text{CuM}^{\text{IIIB}}\text{O}_2$  families so that these materials can be used for their best-suited applications in optoelectronic devices. Furthermore, we need to develop a method to enhance the optical absorption for the Cu delafossite families.

$\text{BiVO}_4$  has shown particular promise for water photodecomposition with the presence of both a low bandgap (2.4–2.5 eV) and reasonable band-edge alignment with respect to the water redox potentials [6]. It has been reported to exhibit both n- and p-type semiconducting properties [7], in addition to high photon-to-current conversion efficiencies. However, to date, the effects of dopants on the electronic properties of  $\text{BiVO}_4$  have not been well explored.

## Approach

We have employed density functional theory (DFT) to study the electronic properties of the delafossite materials and  $\text{BiVO}_4$ . Generalized gradient approximation (GGA) to DFT and the projected augmented wave (PAW) basis as implemented in the Vienna *ab initio* simulation package (VASP) [8] are used. A plane-waves cut-off energy of 400 eV was used, and the ion positions were always relaxed until the force on each of them is 0.01 eV/Å or less. To correct the DFT+GGA underestimation of electron correlation of the cation *d* band, an  $U_{\text{eff}}$  ( $U-J=7$  eV) parameter was added to the DFT Hamiltonian for all the valence Cu-*d*, Sc-*d*, and Y-*d* bands. No *U* was added for the group-III A elements because their filled 3*d* bands are fully occupied shallow core states, which is situated more than 15 eV below the top of the valence band (Al has no *d*-band). Also, we found that adding an additional *U*, for example, on the Ga-3*d* band resulted in a much smaller in-plane lattice *a* parameter compared to the experimental value. In the case of  $\text{CuLaO}_2$ , an empty and highly localized *f*-band is present just above the conduction-band minimum (CBM), and a localized band with *d*-character is seen in the lower edge of the conduction band. This overall presence of *f* on top of *d* character at the CBM makes it particularly sensitive on the choice of *U* parameter in the DFT+*U* scheme. In fact, we found that a small *U* value on the La *d*-band highly overestimates the bandgap relative to experiment. So, for  $\text{CuLaO}_2$ , no *U* potential has been used to La-5*d*. The choice of *U* parameter was not found to affect the relative stability of the hexagonal and rhombohedral delafossite structures. For  $\text{BiVO}_4$ , we found that *U* parameters were not needed.

## Results

We first discuss the structure preferences for the group-III A and -III B delafossites. The delafossite structure can have either  $P6_3/mmc$  (#194) or  $R\bar{3}m$

(#166) space-group symmetry, depending on the stacking sequencing of the O-*M* (*M* = group-III A and -III B) octahedron layers. Our total energy calculation revealed that group-III A delafossites prefer the rhombohedral group ( $R\bar{3}m$ ), whereas group-III B delafossites favor the hexagonal group ( $P6_3/mmc$ ), which is in good agreement with experimental observation. In both symmetries, O and Cu form linear bonding structure along the *c*-axis, which is considered to be the main channel for the hole transport, whereas O-*M* bonds form distorted octahedra.

Figure 1 shows the calculated band structure for the group-III A and group-III B delafossites in rhombohedral and hexagonal structures, respectively. Our results reveal that although the  $\text{CuM}^{\text{IIIA}}\text{O}_2$  and  $\text{CuM}^{\text{IIIB}}\text{O}_2$  delafossites have a similar local structure environment, they have very different electronic properties. Comparing the band structures for the  $\text{CuM}^{\text{IIIA}}\text{O}_2$  and  $\text{CuM}^{\text{IIIB}}\text{O}_2$  delafossites, we find that the nature of the valence band is similar for both group-III A and -III B families. As mentioned earlier, the valence-band maximums (VBMs) are mainly composed of Cu-*d* and O-*p* orbitals. However, for hexagonal  $\text{CuM}^{\text{IIIB}}\text{O}_2$  band structures (lower panel in Figure 1), the occurrence of the VBM at the H point is no longer observable in all cases. For example, for  $\text{CuScO}_2$ , the VBM is still at H-point, but for  $\text{CuYO}_2$  and  $\text{CuLaO}_2$  the VBM appears to be at the  $\Gamma$  point. Larger variations are seen between the CBM of the group-III A and group-III B delafossites.

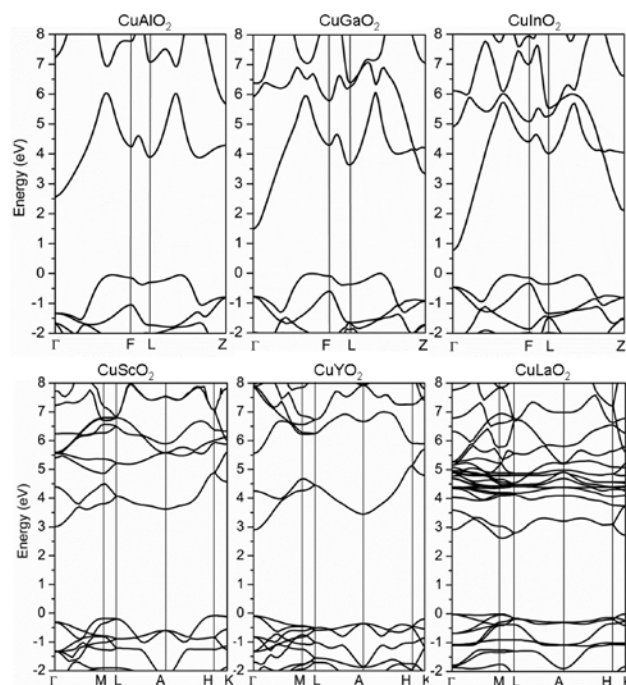


**FIGURE 1.** Calculated electronic band structure of group-III A (upper panel) and group-III B (lower panel) delafossites along the high-symmetry lines of the first Brillouin zone.

The biggest difference is that at the  $\Gamma$  point, the  $s$ -band-derived CBM in the  $\text{CuM}^{\text{IIIB}}\text{O}_2$  family is not as deep as compared to that in the  $\text{CuM}^{\text{IIIA}}\text{O}_2$  family. First, comparing the band structure of  $\text{CuScO}_2$  and  $\text{CuGaO}_2$ , we clearly see the much lower CBM due to Ga-4s band in the later at  $\Gamma$  point. For  $\text{CuScO}_2$ , the presence of unoccupied Cu-3d states at the CBM ( $\Gamma$  point) makes it much less dispersive. Secondly, for Ga, all its 3d bands are occupied and are situated at much higher binding energy below the Fermi level, and they do not contribute much to the conduction band. At the L point, significant Ga- $s$  contribution along with  $p$  character is seen for  $\text{CuGaO}_2$ . In contrast, for  $\text{CuScO}_2$ , the  $d$  contribution is significant at the L point of the conduction band because of its partially filled Sc-3d nature. In addition, unoccupied  $f$  bands are present in the conduction band in  $\text{CuLaO}_2$ , which affect the CBM significantly. In principle, all the differences identified above can be attributed to the differences in electronic configurations between group-IIIA and -IIIB elements. The detailed discussions can be found in Ref. [9]. Our results explain well the experimentally reported bandgap trends for  $\text{CuM}^{\text{IIIB}}\text{O}_2$  delafossites.

We have also calculated the optical transition matrix elements for the band edges of group-IIIB delafossites at the special symmetry points as shown in Figure 1. Only the diagonal components (direct gap) of the momentum matrix were calculated, because the off-diagonal elements would not contribute significantly to optical absorption. In all cases, the transition between VBM and CBM at the  $\Gamma$  point is forbidden (zero transition matrix elements), because of mainly  $d$  character for both VBM and CBM and transition would result in a parity violation. Therefore, for the application for PEC water splitting, Cu delafossites have too weak absorption, particularly for visible light.

The zero contribution to the optical absorption at the  $\Gamma$  point is due to the inversion symmetry of the delafossite structure. For efficient PEC water splitting, the optical absorption of Cu delafossites must be enhanced significantly. We found that significant band-structure modification can be achieved by isovalent alloying of Cu-based delafossites. This alloying significantly improves the optical absorption at lower energy because it reduces the crystal symmetry; thus, it lifts the parity-forbidden transition near the band edge, which exists in the pure delafossite compounds. Moreover, the bandgap of the quaternary delafossite alloy can be further tuned through alloy composition and ordering, thus improving the flexibility in designing delafossite-based PEC photo-electrodes. Figure 2 shows a few examples of mixed Cu delafossites. Figure 2(a) shows the structure of  $\text{Cu}(\text{Y,Ga})\text{O}_2$ , where Ga substituted at Y site with a 1:1 ratio. The crystal structure (type-I), Ga- and Y-based octahedrons are separated by the O-Cu-O chain, i.e., Ga and Y are not present in the same octahedron layers. Figure 2(b)

shows the structure (type-II) with the same composition of the structure shown in Figure 2(a). However, Ga and Y are present in the same octahedron layers. Figure 2(c) shows the structure of  $\text{Cu}(\text{Y,Ga,In})\text{O}_2$ , where the ratio of Y:Ga:In is 2:1:1.

Figure 3 shows the calculated optical absorption coefficient for the three isovalent alloys. For comparison, the optical absorption coefficient of pure  $\text{CuYO}_2$  is also given. Due to this mixed nature of the CBM, the transition matrix element is no longer zero. However, the matrix element is still not very large because for this isovalent alloy, the wavefunction mixing is relatively small. Nevertheless, the breakdown of the inversion symmetry should help to improve the near-band-edge absorption. The 50%-50% alloy, however, has an indirect bandgap with its VBM away from  $\Gamma$ , which may not be desirable for PEC application. However, this can be remedied by further band engineering, e.g., by reducing the Ga concentration. The absorption onset

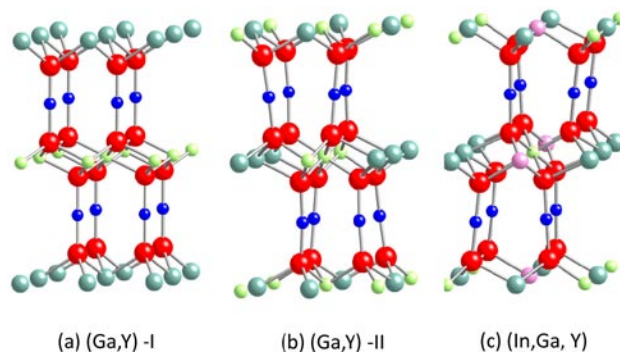


**FIGURE 2.** Atomic structures of mixed  $\text{Cu}(\text{Y,Ga})\text{O}_2$  delafossite, where Y and Ga atoms (a) are in different planes and (b) share the same plane; (c) mixed  $\text{Cu}(\text{Y,Ga,In})\text{O}_2$  structure, where the ratio of Y:Ga:In is 2:1:1.

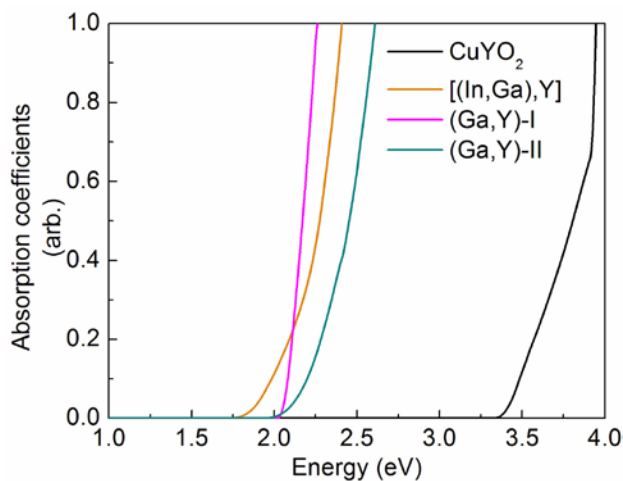


**FIGURE 3.** Calculated absorption coefficients for different alloys and pure  $\text{CuYO}_2$ .

of the type-II alloy is slightly lower in energy; however, the absorption increase is faster for the type-I layer structure, and both show remarkable improvements over bulk  $\text{CuYO}_2$ . The direct bandgap for  $\text{Cu}(\text{Y,Ga,In})\text{O}_2$  at  $\Gamma$  point is 1.725 eV. Close inspection of the absorption curve also shows the onset of absorption at the same energy. This indicates that first, the bandgap is reduced further from the type-I and type-II alloys, and second, the absorption at the  $\Gamma$  point is not suppressed.

$\text{BiVO}_4$  is a promising photocatalyst for hydrogen generation, with demonstrated experimental potential in terms of bandgap, stability, and conductivity. Recent experiments have shown that doping of W can significantly enhance the PEC performance of  $\text{BiVO}_4$  [10]. Therefore, we have calculated the doping effects of W in  $\text{BiVO}_4$ .

Figure 4 shows our preliminary results of doping of W in  $\text{BiVO}_4$ . Figure 4(a) shows the calculated band structure of a  $\text{BiVO}_4$  supercell with one W at a V site. We found that the band structure is very similar to that

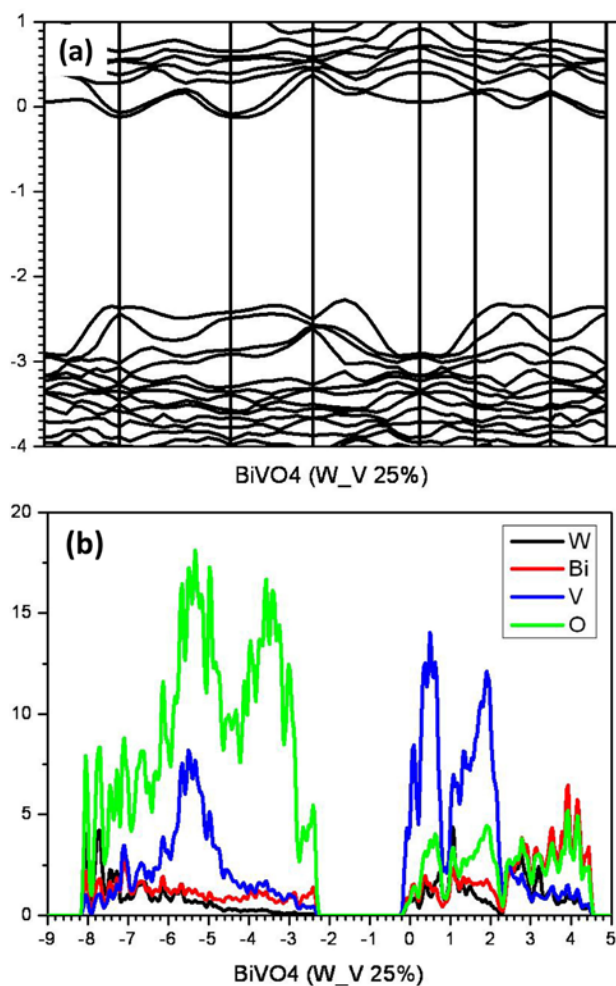


**FIGURE 4.** Calculated band structure (a) and site projected density of state (b) for W-doped  $\text{BiVO}_4$ .

of pure  $\text{BiVO}_4$ , indicating that substitutional W at V sites do not create any deep level in the bandgap and the W s states are much higher in energy than the CBM. This is seen in the site projected density-of-state plot shown in Figure 4(b). These results indicate strongly that substitutional W atoms at V sites are degenerate donors, which are the most preferred donor states. We have also considered substitutional W atoms at Bi sites. We found that they are also shallow donors. However, our preliminary results indicate that W prefers the V site more than Bi due to better atomic size matching.

## Conclusions and Future Directions

We have calculated the electronic structure of Cu delafossites and W doping in  $\text{BiVO}_4$  using DFT. We have provided a detailed understanding on the different electronic structure for group-IIIA and group-IIIB delafossites. We have understood why the Cu delafossites have insufficient optical absorption in the visible-light regime, and we have demonstrated that significant bandgap modification can be achieved by isovalent alloying of Cu-based delafossites. This alloying significantly improves the optical absorption at lower energy because it reduces the crystal symmetry, thus lifting the parity-forbidden transition near the band edge, which exists in the pure delafossite compounds. Moreover, the bandgap of the quaternary delafossite alloy can be further tuned through alloy composition and ordering, thus improving the flexibility in designing delafossite-based PEC photo-electrodes. Our preliminary results have shown that W doping in  $\text{BiVO}_4$  may enhance the n-type conductivity. In future study, we will provide a detailed understanding of defect physics in  $\text{BiVO}_4$ , including the formation energies and transition energies of intrinsic and extrinsic defects.

Future directions will include the following:

- Perform a detailed study of defect physics in  $\text{BiVO}_4$ .
- Design new metal oxides with desirable optical absorption, band-edge positions, and transport properties.
- Extend our study to non-oxide materials, such as nitrides, carbides, and sulfides.

## FY 2010 Publications/Presentations

1. Muhammad N. Huda, Yanfa Yan, Aron Walsh, Su-Huai Wei, and Mowafak M. Al-Jassim, "Symmetry-breaking-induced enhancement of visible light absorption in delafossite alloy," *Appl. Phys. Lett.* **94**, 251907 (2009).
2. Muhammad N. Huda, Yanfa Yan, Aron Walsh, Su-Huai Wei, and Mowafak M. Al-Jassim, "Group-IIIA versus IIIB delafossites: Electronic structure study," *Phys. Rev. B* **80**, 035205 (2009).

3. Muhammad N. Huda, Aron Walsh, Yanfa Yan, Su-Huai Wei, and Mowafak M. Al-Jassim, "Electronic, structural, and magnetic effects of 3d transition metals in hematite," *J. Appl. Phys.* **107**, 123712 (2010).

4. Yanfa Yan, Wan-Jian Yin, M.M. Al-Jassim, and John Turner, "Doping of BiVO<sub>4</sub>" 2010 DOE Hydrogen Production Working Group Meeting, Las Vegas.

## References

1. M. Younsi, S. Saadi, A. Bouguelia, A. Aider, and M. Trari, *Sol. Energy Mat. Sol. Cells* **91**, 1102 (2007).

2. S. Saadi, A. Bouguelia, A. Derbal, and M. Trari, *J. Photochem. Photobiol. A: Chem.* **187**, 97 (2007).

3. J. Pellicer-Porres, A. Segura, A.S. Gilliland, A. Muñoz, P. Rodríguez-Hernández, D. Kim, M.S. Lee, and T.Y. Kim, *Appl. Phys. Lett.* **88**, 181904 (2006).

4. S. Gilliland, J. Pellicer-Porres, A. Segura, A. Muñoz, P. Rodríguez-Hernández, D. Kim, M.S. Lee, and T.Y. Kim, *Phys. Stat. Sol. (b)* **244**, 309 (2007).

5. B.J. Ingram, G.B. Gonzalez, T.O. Mason, D.Y. Shahriari, A. Barnabe, D. Ko, and K.R. Poeppelmeier, *Chem. Mater.* **16**, 5616 (2004).

6. K. Sayama, A. Nomura, T. Arai, T. Sugita, R. Abe, M. Yanagida, T. Oi, Y. Iwasaki, Y. Abe, and H. Sugihara, *J. Phys. Chem. B* **2006**, *110*, 11352.

7. I.C. Vinke, J. Diepgrond, B.A. Boukamp, K.J. de Vries, and A.J. Burggraaf, *Solid State Ionics* **57**, 83 (1992).

8. G. Kresse and J. Furthmüller, *Comput. Mater. Sci.* **6**, 15 (1996).

9. M.N. Huda, Y. Yan, A. Walsh, S.-H. Wei, and M.M. Al-Jassim, *Phys. Rev B* **80**, 035205 (2009).

10. S.F. Sameera, P.P. Rao, L.S. Kumari, and P. Koshy, *Chemistry Letters* **38**, 1088 (2009).